MODELING AND ANALYSING FOR WRITING ROBOT ARM

Xu XIAOFEI[1], Yang SHUHUI[2], Li DENGHUA[3]

Servo motor driver was a new kind of driving way which could realize continuous writing character according to the expected rule. In order to improve controlling precision of the continuous writing arm the stability speed and position, it was important to establish accurate mathematical model of the system. Firstly the kinematics and dynamics model of servo motor was identified in the experiment, then the mathematical and state equation model of information transmission mechanism parts were derived and established. Then the established model was verified by comparing with the output of the implementation system, which an adaptive controller of RBF neural network was proposed according to the collected sample data, and the results of writing special Chinese characters fitting precision could be reached to 94%.The simulation and test result were shown that the writing robot was controllable.

Keywords: Modeling; Error Analyzing; Writing Robot; Position Control Method; Coordinate Transformation

1. Introduction

The stability and convergence of the industrial robot was dependent on the neural network and adaptive control algorithm, which was improved by the calculation and application of convergence of some special differential equations modeling [1]. The robot kinematic parameters and error calibration were researched by measuring instruments cooperation target [2], or imposed spatial constraints on the robotic end effect, or optimized by the Barbalat [3] of Lyapunov analysis [4]，Global invariant set theorem [5]，Inequality analysis method [6]，which was satisfied with approximation effect on the Neural network parameters constraints. Some considerable aspects existing in the researches were also pointed out, that the method above could only be realized in the good region limited the adaptive Neural network accuracy [7-9], because nonlinear algorithm could speed up learning and avoid effectively local minimization problem to track set movement trajectory.

[1] School of Electronic and Information Engineering, Beijing Jiaotong University, Beijing, 100044, China; E-mail: 18910782910@163.com
[2] School of Information Engineering, Communication University of China, Beijing 100024, China;
[3] School of Automation, Beijing Information Science and Technology University, Beijing, 100192, China

The paper discussed system response characteristics of the robot joint angle trajectory tracking servo position control problem and the definition of the kinematics and dynamics model on the writing robot mechanical arm were based on the D-H model to estimate some position error [10-11]. Based on adaptive robust control law and with RBF neural network approximate adaptive robust control strategy, the writing robot controller had been built, consisting of a four or six DOF(degrees of freedom) master micro actuator joint, which could be designed and adjusted the deviation of the location of controllable terminal to receive instruction, examine data, feedback information and output control signal, and the implemented writing robot could meet their final destinations to write special recognizable Chinese characters. Writing robot was a typical nonlinear, multi variable, strong coupling and naturally unstable system to be studied further [12-17].

2. The Prototype of Writing Robot

There was the principle Mechatronics information flow scheme diagram of design of writing robot system in Fig.1, which was generally divided into two parts, the first part from the writing instruction information sender, and the second part from the writing instruction information receptor. The part1 included three kinds of writing instruction sending mode: In solution1, the writing instruction was set in the controller; in solution2, the writing instruction was set by wearing a data glove; in solution3, the writing instruction was set in software from host compute. The upper computer of the writing robot had the hierarchical Chinese character database based on radical reuse, according to specific Chinese characters writing tasks, so the tip movement followed the order to obtain a suitable value from top to bottom, from left to right and left on the starting point.

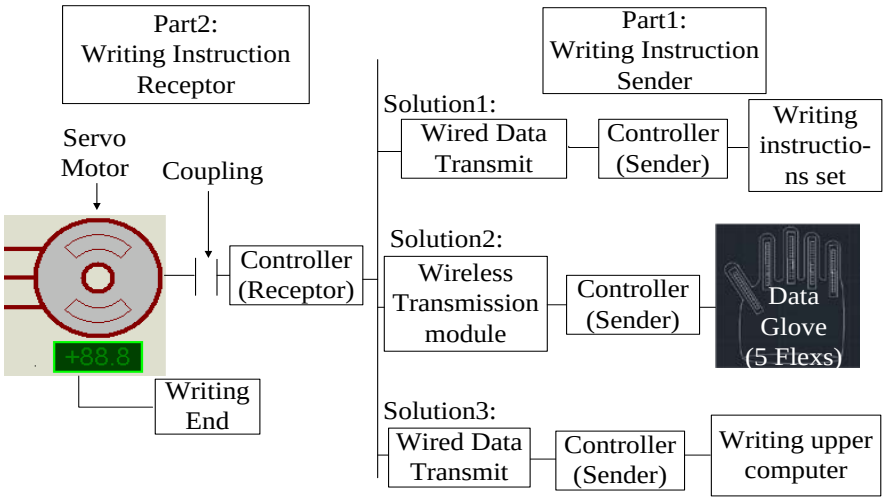

Fig.1 The principle Information Flow Scheme of the Designed Mechatronic System on Writing Robot

3. Design the Model of Writing Robot

3.1 The Kinematics Model

Through using the D-H method, the basic simulation and functions in the upper software were to build coordinate systems on all parts of writing robot arm, and define other parameters. So the work had been completed the analysis of forward kinematics and inverse kinematics of the writing robot arm, to get the transformation matrix between the body and the foot coordinate system in the main.

3.1. 1 the Forward Kinematics Model

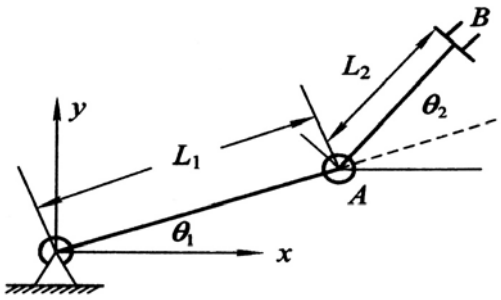

Fig.2 the length and geometric parameters of the joint

As shown in Fig.2, connecting the two link rod lengths L_1 and L_2, and

define vectors $\boldsymbol{R}$ and $\boldsymbol{\theta}$ for terminal position and joint variables at the end of the robot arm:

$$\boldsymbol{R} = [x,\ y]^{\mathrm{T}},\ \boldsymbol{\theta} = [\theta_1,\ \theta_2]^{\mathrm{T}},\ \boldsymbol{R} = \boldsymbol{f}(\boldsymbol{\theta}) \tag{1}$$

Among them, x and y are the coordinates of the end of the manipulator in the xoy coordinate system, θ_1 and θ_2 were the rotation angles of the two links, and there was not hard to conclude the following equation:

$$x = L_1\cos\theta_1 + L_2\cos(\theta_1+\theta_2) \tag{2}$$

$$y = L_1\sin\theta_1 + L_2\sin(\theta_1+\theta_2) \tag{3}$$

Moreover, if given the more rotation angles θ_i of the links, the position equation of the forward kinematics manipulator end could be obtained by multiplying the transformation matrix of each link.

3.1.2. The inverse kinematics model

As shown in Fig.3, connecting the two link rod lengths L_1 and L_2, and assuming the terminal position $\boldsymbol{B}$（x，y）and vectors $\boldsymbol{\theta}$ of the robot arm:

Among them, x and y were the coordinates of the end of the manipulator in the xoy coordinate system, θ_1 and θ_2 were the rotation angles of the two links, and according to the geometric relations of △AOB, and the vector α *was* obtained by cosine theorem:

$$\alpha = \arccos((L_1^2 + L_2^2 - (x^2 + y^2))/2\ L_1\ L_2) \tag{4}$$

then,

$$\theta_2 = \pi - \alpha \tag{5}$$

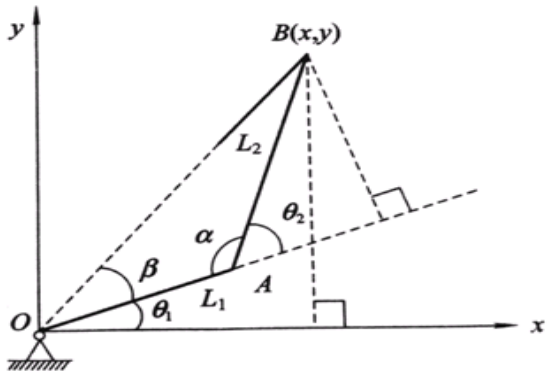

Fig.3 the length and geometric parameters of the joint

Here,

$$\tan(\beta + \theta_1) = y/x \tag{6}$$

$$\beta + \theta_1 = \arctan(y/x) \tag{7}$$

and,

$$\text{Tan}\beta = L_2\sin\theta_2/(L_1 + L_2\cos\theta_2) \quad (8)$$

$$\text{So,} \quad \beta = \arctan(L_2\sin\theta_2/(L_1 + L_2\cos\theta_2)) \quad (9)$$

$$\text{Then } \theta_1\text{: } \theta_1 = \arctan(y/x) \ -\arctan(L_2\sin\theta_2/(L_1 + L_2\cos\theta_2)) \quad (10)$$

Moreover, if given the more rotation angles θ_i of the links, the position equation of the forward kinematics manipulator end could be obtained by multiplying the transformation matrix of each link, and the positive motion equation of the previous section was represented by [RHS].

3.2 The dynamics model

The schematic of writing robot kinematics system was essentially the analysis actuator position control, as shown in Fig.5. The work was established the electromechanical-coupled actuator kinematic model of a novel writing robot, and the plan of actuator drive voltage control was discussed. The dynamic model was focused on the mechanical analysis of the friction, analyzing the power loss to search the feedback loops of a system, as shown in Fig.4:

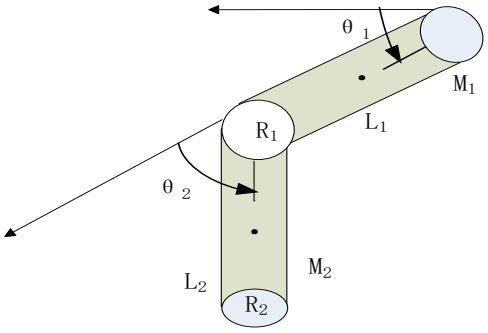

Fig.4 the kinematic model of actuator link

Using Lagrange-Euler and Newton-Euler method, the general dynamic equation of the robot could be obtained. Fig.4 showed the writing arm of a writing robot with a steering knuckle composed of a two actuator links. The corresponding dynamic equations (including the load and friction terms) were as follows:

$$
\begin{aligned}
p_1 &= \left[\frac{1}{4}(\mathrm{M_1R_1^2}+\mathrm{M_2R_2^2})+\frac{1}{3}(\mathrm{M_1L_1^2}+\mathrm{M_2L_2^2})+\mathrm{M_2L_1^2}+\mathrm{M_2L_1L_2}\cos\theta_2\right]\ddot{\theta}_1 \\
&+\left[\frac{1}{4}\mathrm{M_1R_2^2}+\frac{1}{3}\mathrm{M_2L_2^2}+\frac{1}{2}\mathrm{M_2L_1L_2}\cos\theta_2\right]\ddot{\theta}_2-\frac{1}{2}\mathrm{M_2L_1L_2}\sin\theta_2\dot{\theta}_2 \\
&-M_2\mathrm{L_1L_2}\dot{\theta}_1\dot{\theta}_2\sin\theta_2+\frac{1}{2}\mathrm{M_2L_2}g\cos(\theta_1+\theta_2)+(\frac{1}{2}\mathrm{M_1}+\mathrm{M_2})\mathrm{L_1}g\cos\theta_1 \\
&+\nu_1\dot{\theta}_1+\mathrm{L_1}\sin\theta_2 f_x+(\mathrm{L_2}+\mathrm{L_1}\cos\theta_2)f_y+n_x
\end{aligned}
\tag{11}
$$

$$
\begin{aligned}
p_2 &= (\frac{1}{4}\mathrm{M_2R_2^2}+2\mathrm{M_2L_1L_2}\cos\theta_2+\frac{1}{3}\mathrm{M_2L_2^2})\ \ddot{\theta}_1+(\frac{1}{4}\mathrm{M_1R_2^2}+\frac{1}{3}\mathrm{M_2L_2^2})\ \ddot{\theta}_2 \\
&+\frac{1}{2}\mathrm{M_2L_1L_2}\dot{\theta}_1^2\sin\theta_2+\frac{1}{2}\mathrm{M_2L_2}g\cos(\theta_1+\theta_2)+\nu_1\dot{\theta}_2+\mathrm{L_2}f_y+n_y
\end{aligned}
\tag{12}
$$

Here, $\theta_1(t)$ or $\theta_2(t)$ was the actuator position angle, $p_1(t)$ or $p_2(t)$ was the actuator position torque, M_1 or M_2 was the mass of force arm, and all the quality assumptions was focused on the center of the arm. From the dynamic equations (36) - (37), it could be seen that the dynamic characteristics of the system were nonlinear and coupling, too difficult to calibrate. The friction calculating was important for dynamic calculating model analysis, especially for response analysis.

3.3 The Basic Model

3.3.1 The Basic Model of the Pen

The research of writing robotic technology was mainly centralized in system structure, which the upper computer was created and modified the Chinese or English character vector data. The validity of the designed algorithm was verified with MATLAB and the algorithm was simulated with MODELSIM; so the physical system controller, based on the theory of control and simulation software, had been designed by the method of parameter extraction. Writing robot manipulator were composed of a four DOF master micro actuator joint to controlling the pen, and the joints Modeling using Robotics Toolbox manipulator were the rotating joint, the slider to generate a range of writing for each degree of freedom manipulator model, as shown in Fig.5(a).

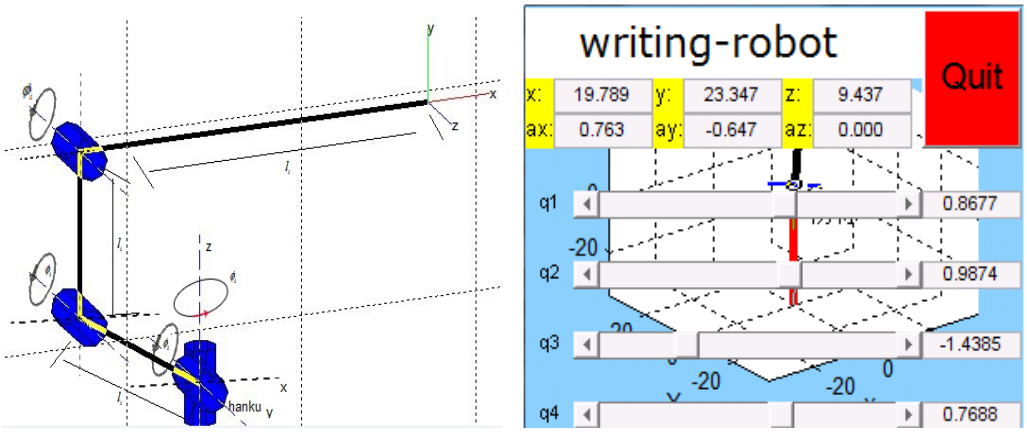

(a) Actuator Model (b) Verification model

Fig. 5 Construction and Verification of Manipulator Arm Model

And in Fig.5 (b), the definition of robot essential operations were performed on objects to define in a D-H coordinate system, which were translation, rotation, and scaling to calculate actuator position error. For the design involved 4 or 6 degrees of freedom manipulator, the actuator position end was given to solve each joint, and each joint actuator end coordinate could correspond with many different joint angles, so the inverse solution was not the only one. As shown in Fig.5, the spread value was 9.437 during writing "writing-robot", which could be very close to the ideal results. As shown in Table 1，the D-H coordinate parameters were created，and the variation range of each link angle was determined $-90^{\circ} \le \theta_1, \theta_2, \theta_3, \theta_4 \le 90^{\circ}$:

Table 1

D-H parameters

Link i	l_i (cm)	θ_i ($^{\circ}$)	Initial phase
1	8	0	0
2	8	-50	-pi/4
3	8	50	-pi/4
4	20	90	pi/8

3.3.2 The Basic Model of the Brush

Writing robot manipulator was composed of six DOF master micro actuator joint to control the brush, which the translation, rotation, and scaling technique were harder than to control the brush for stable and different font style,

as shown in Fig.6.

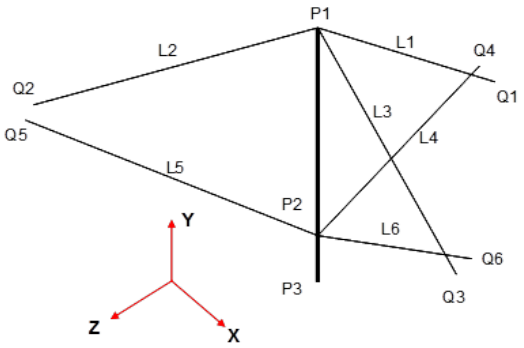

Fig.6 Brush robotics model

In this model, the position of the support point Q_1~Q_6 of the 6 ropes was fixed and known. Meanwhile, the relative positions of the two control points P_1,P_2 of the brush, and the brush point P_3 remain unchanged. The position and orientation of the brush were described by the coordinates of P_2 points（X_{P2}，Y_{P2}，Z_{P2}）and the unit vectors (i，j，k）of the line in which the brush was located. The coordinates of the P2 points were known, and the coordinates of the P_1 point was:

$$\begin{cases} X_{P1} = X_{P2} + i \times L_{P1P2} \\ Y_{P1} = Y_{P2} + j \times L_{P1P2} \\ Z_{P1} = Z_{P2} + k \times L_{P1P2} \end{cases} \tag{13}$$

Using the coordinates of two points P_1,P_2 and six points Q_1~Q_6 in the Fig.4,the six lengths of the ropes could be gained,then put the length of 6 ropes $L_1 = L_2 = L_3 = L_U$， $L_4 = L_5 = L_6 = L_D$ into the formula (10):

$$\theta_i = \theta_0 + (L_i - L_u) \times 180° / \pi R, (i = 1,2,3,4,5,6) \tag{14}$$

$$\begin{cases} \theta_1 = \theta_0 + (L_1 - L_u) \times 180° / \pi R \\ \theta_2 = \theta_0 + (L_2 - L_u) \times 180° / \pi R \\ \theta_3 = \theta_0 + (L_3 - L_u) \times 180° / \pi R \\ \theta_4 = \theta_0 + (L_4 - L_D) \times 180° / \pi R \\ \theta_5 = \theta_0 + (L_5 - L_D) \times 180° / \pi R \\ \theta_6 = \theta_0 + (L_6 - L_D) \times 180° / \pi R \end{cases} \tag{15}$$

Here, θ_0 was 150° and R was the radius of the winding circumference, and L_i was the length of the rope. The length of the L_{p1p2} =

$|P_1P_2|$=180 mm，and the six point coordinates (unit mm) was:

Q_1(7.5,105.5,-174.7); Q_2(-155.08,105.5,80.87); Q_3(147.58,105.5,93.68);

Q_4(-7.5,105.5,-174.74); Q_5(-147.58,105.5,93.68); Q_6(155.08,105.5,80.87)

Other parameters was：L_U = 209.045mm, L_D = 186.671mm,R = 37.5mm.

4. Simulation and Analysis

4.1 The Control Tactic for System

For an input vector $X=[x_1,x_2,\cdots x_d]^T\in R^d$,the output of the last hidden layer node $o_i(i=1,2,\cdots m)$,the output of the neural network $Y=[y_1,y_2,\cdots y_c]^T$:

$$y_i=\omega_{\sigma i}+\sum_{j=1}^{M}\omega_{ij}o_j=\omega_{\sigma i}+\sum_{i=1}^{N}\omega_i\varphi(\|x-x_i\|) \tag{16}$$

Here,$\{\varphi(\|x-x_i\|)\,|\,i=1,2,\cdots,N\}$ was a collection of N arbitrary radial basis functions, $\|\bullet\|$ represented the norm, the training data, as the radial basis function center； $\omega_{\sigma i}$ was the offset from i output nodes, and ω_{ij} was the weights of the second linear equality, from j hidden nodes to i output nodes:

$$\begin{bmatrix}\varphi_{11} & \varphi_{12} & \cdots & \varphi_{1N}\\ \varphi_{21} & \varphi_{22} & \cdots & \varphi_{2N}\\ \vdots & \vdots & & \vdots\\ \varphi_{N1} & \varphi_{N2} & \cdots & \varphi_{NN}\end{bmatrix}\begin{bmatrix}\omega_1\\ \omega_2\\ \vdots\\ \omega_3\end{bmatrix}=\begin{bmatrix}y_1\\ y_2\\ \vdots\\ y_3\end{bmatrix} \tag{17}$$

$$\varphi_{ij}=\varphi(\|x_j-x_i\|),(j,i)=1,2,\cdots N \tag{18}$$

Gauss (Gauss) function satisfies Micchelli theorem, which was characterized in that the number of hidden nodes to be equal to the number of input samples:

$$\varphi(r)=\exp(-\frac{r^2}{2\sigma^2}) \tag{19}$$

Here,σ was the width value of basic function, it could be seen that the width of the radial basis function was smaller, and the selectivity was stronger.

For the output sample *T*,the mean square error function of the neural network learning was *E*:

$$E=\frac{1}{n}\sum_{j=1}^{n}\sum_{i=1}^{c}(t_i-y_i)^2 \tag{20}$$

In the simulation program, the initial position and orientation of the

inverse and forward kinematics problem were defined firstly q_i, which could be deduced from equation(37):

$$D(q)\ddot{q} + C(q,\dot{q})\dot{q} + G(q) = \tau + d \tag{21}$$

There: $$D(q) = \begin{bmatrix} v + q_{01} + 2\gamma\cos(q_2) & q_{01} + q_{02}\cos(q_2) \\ q_{01} + q_{02}\cos(q_2) & q_{01} \end{bmatrix} \tag{22}$$

$$C(q,\dot{q}) = \begin{bmatrix} -q_{02}\dot{q}_2\sin(q_2) & -q_{02}(\dot{q}_1 + \dot{q}_2)\sin(q_2) \\ q_{02}\dot{q}_1\sin(q_2) & 0 \end{bmatrix} \tag{23}$$

$$G(q) = \begin{bmatrix} 15g\cos q_1 + 8.75g\cos(q_1 + q_2) \\ 8.75g\cos(q_1 + q_2) \end{bmatrix} \tag{24}$$

There: v=13.33, q_{01}=8.98, q_{02} =8.75,g=9.8

The error disturbance，the position command and the initial state of the system were: $d_1 = 2, d_2 = 3, d_3 = 6$

Location instruction:

$$\begin{cases} q_{1d} = 1 + 0.2\sin(0.5\pi t) \\ q_{2d} = 1 - 0.2\sin(0.5\pi t) \end{cases} \tag{25}$$

The initial value of the controlled object was $[q_1 \quad q_2 \quad q_3 \quad q_4] = [0.6 \quad 0.3 \quad 0.5 \quad 0.5]^T$, and the 20% change of $\Delta D, \Delta C, \Delta G$.

In the simulation program, the adaptive law was adopted as the default，$\gamma = 20, k_1 = 0.001$，and the adaptive control rate was controlled by neural network with the original BH joint rotation angle Q the same numerical:

$$Q = \begin{bmatrix} 50 & 0 & 0 & 0 \\ 0 & 50 & 0 & 0 \\ 0 & 0 & 50 & 0 \\ 0 & 0 & 0 & 50 \end{bmatrix} \tag{26}$$

The initial values of the Koski function parameters were taken $[-2 \quad -1 \quad 0 \quad 1 \quad 2]$ and 3 respectively.

The learning samples of 125 sets of data were obtained from link space $Q = \{\theta_1, \theta_2, \theta_3, \theta_4\}$ and the corresponding spatial position $P = \{p_x, p_y, p_z\}$, when the adaptive RBF network error objective (goal) was 0.01,and the spread constant (spread) of the radial basis neuron layer was 1.25，the results compared

with the actual data, the absolute error was small.

4.2 System implementation and trajectory analysis

There were two entire assemble writing robots of the physical mechanical arm system to meet the trajectory constraint，which the experiment was created by author team and done with a controller and a plurality of servo series such as shown as a proof-of-concept prototype in Fig.7. The pen is attached (in Fig. 7a) to the robot arm using a handle fixing, and in Fig.7b the brush is connected to flexible plastic wires, which are very elastic transmission and affect the repeatability. Next step, a better choice is well-considered to use steel kernel wires (like wires from desk- plotters), which the product will be highlights the quality and value, and indomitableness.

(a) The photo of 4 DOF pen writing robot (b) The photo of 6 DOF brush writing robot

Fig.7 writing robotics system of author team

Each had distinct advantages and disadvantages to simulate the complex human writing Chinese characters control behavior, namely the tip trajectory problem could be established. There were a soft key for upper controller, once pressed, set the timer going and showing, which was measured/detected controller delay of less than 5 seconds.

The internal control voltage curves change with time, the target value and actual tracking value were uniform characteristics, as shown in Fig.8.

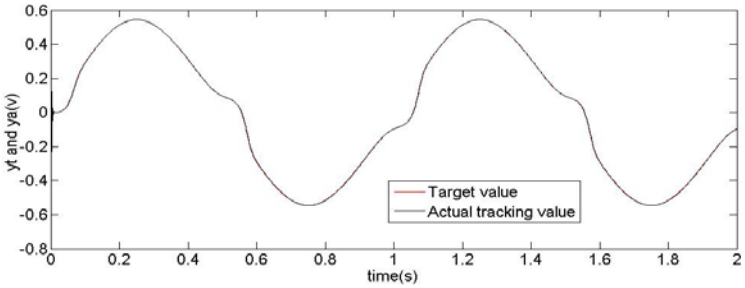

Fig.8 The internal control voltage curves change with time

The error of controlling writing robot's different link position was indicated in Fig.9. The research on the links angle servo control effect of friction actuator angle tracking position control was shown in contrast curves data of the target value and the actual value, which the error was caused by the control delay and fault of slight fluctuations, such as signal conditioning circuit noise. In Fig.9 (b), the error was more close to zero beyond less time for series attenuation.

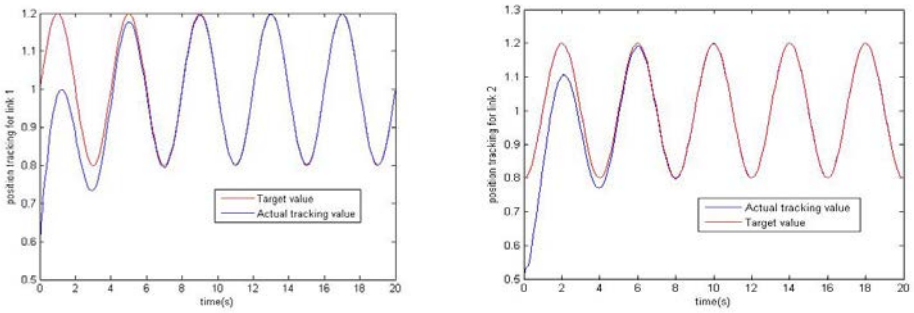

(a) Position tracking for first link (b) Position tracking for second link

Fig.9 The position curves change with time

This experiment was done in the same pen writing robot, which were created by author team. The differences of force output between tip friction and link torque was indicated in Fig.10. The research on tip friction and link torque was shown in the force curves change with time, which the error decided the controller output driving voltage next step. From the chart, maximum and random difference value could clearly be seen on the crucial opening seconds, and the abscissa was the response time, while that of later time was more identical.

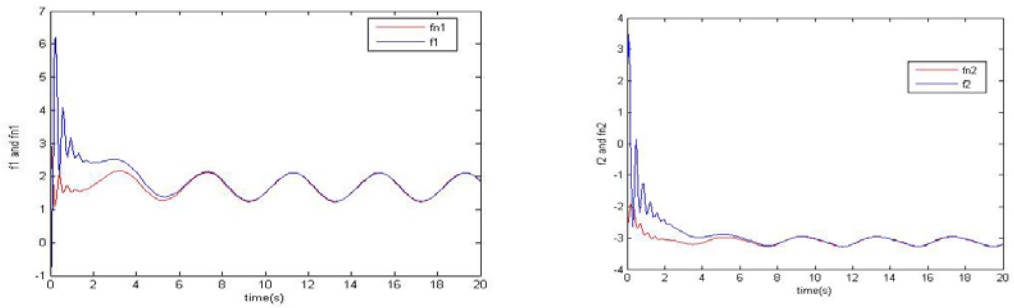

(a) The contrast force curves between tip friction f_1 and first link torque f_{n1} (b)The contrast force curves between tip friction f_2 and second link torque f_{n2}

Fig.10 The force curves change with time

Ultimately, the factors of resulting in the main error were found from the inertia, velocity, and the tip signal conditioning circuit noise, sampling frequency. A signal proportional to the actuator position was obtained and filtered from the incremental or absolute angular encoders and so on, which will be an improvement goal for further research.

5. Conclusion

The adaptive neural network control algorithm had been realized to reduce the uncertainty and error of approximation, and develop the convergence of the writing manipulator in the paper; During the process of writing and power transmission of the mechanical arm, the sliding friction between the tip end and paper were the main factor of affecting the control precision, which made limit cycles and the tracking error for the output of the system; Due to the neural network can be approximate for any nonlinear continuous function with arbitrary precision, as we all have been known, the research will be great potential to solve the problem of tracking error writing manipulator; The next step, first before the self-adaptive calculation, the initial value which combines the target with the measured information can be got by using the coiling Chinese character fonts design data model; So it will be to further simplify the complexity of neural network control, within the premise of writing accuracy of target unchanged, with less parameters to improve the stability of N joints robot manipulator system of writing, so that the actual position of the end of the near future expectation value.

Through the simulation and experimental results in the paper, the control strategy of writing robot terminal stability control system was developed with the increase of actuator speed. The motion mathematics characteristic of internal classic model on the force and torque was analyzed to make the actual tip position close to the desired value. Experimental and simulation results were consistent, which the terminal executions end and upper controller delay was less than 5 seconds; at the same time, the recognition degree of font structure shape was high, which can be satisfied with the design index. The control strategy would be applied to the multi-DOF servo control system in general.

R E F E R E N C E S

[1]. *Feng G.* A compensating scheme for robot tracking based on neural networks. Robotics and Autonomous Systems, 1995, 15:100-106

[2] *Ge S S, Lee T H, Harris C J.* Adaptive Neural Network Control of Robotic Manipulators. World Scientific, London, 1998

[3] *Ge S S, Hang C C,Woon L C.* Adaptive Neural Network Control of Robotic Manipulators in Task Space. IEEE Transactions on Industrial Electronics, 1997, 44(6): 746-752

[4].*Xuxiaofei* et al. Structure and motion design of humanoid robot. ELECTRONIC TECHNOLOGY 2015:23-27

[5] *Xuxiaofei* et al. Intelligent Robot [M]. Tsinghua University press, 2016:47-66

[6]. Xuxiaofei et al. Cymbal Piezoelectric Composite Transducer for Soccer Robot Attitude Detection Application. 2014 Applied Mechanics and Materials (ISSN: 1662-7482)(EI)

[7]. *Xia T, Sun H Y, Fan J Zh, et al.* Research of industrial robot calibration based on virtual closed kinematic chain. Machine Design Research, 2009, 25(2):57-59.

[8]. *Li T, Sun K, Jin Y, et al.* A novel optimal calibration algorithm on a dexterous 6 DOF serial robot with the optimization of measurement poses number [C] Robotics and Automation (ICRA), 21international Conference on. IEEE, 2011: 975-981.

[9]. *Chiu C S, Lian K Y, Wu T C.* Robust adaptive motion/force tracking control design for uncertain constrained robot manipulators . Automatica, 2004, 40: 2111-2119.

[10]. *Kwan C M, Yesildirek A, Lewis F L.* Robust force/motion control of constrained robots using neural net network. Journal of Robotic Systems, 1999, 12(16):697-714.

[11]. *Mostefai L, Denai M, Hori Y.* Robust tracking controller design with uncertain friction compensation based on a local modeling approach. Mechatronics, IEEE/ASME Trans. 2009, 15: 746-756.

[12]. *Bakur Alqaudi, Hamidreza Modares, Isura Ranatunga, Shaikh M Tousif, Frank L Lewis, Dan O Popa*. Model reference adaptive impedance control for physical human-robot interaction. Control Theory and Technology.2016, (1)

[13]. *Zoe D, Suguru A.* A position/force control for a robot finger with soft tip and uncertain kinematics. Journal of Robotic Systems, 2002, 44(4):115-131.

[14]. *Hinton G E,Osindero S,The Y W.* A fast learning algorithm for deep belief nets. Neural Computation, 2006, 18(7):1527-1554

[15]. *Kim,B.S. and Calise, A.J.* Nonlinear Fight control using neural networks. Journal of Guidance Control and Dynamics.1997, 20(1):66-70.

[16]. Zhang *Wei-Cun, Liu Ji-Wei, Hu Guang-Da.* Stability analysis of robust multiple model adaptive control systems. Acta Automatica Sinica, 2015, 41(1) 113-121

[17]. *Zhang Sh Zh, Rong W B, Tai G A, et al.* Designing and Dynamic Modeling of 1D Nano-positioner Based on Stick-slip Motion Principle. Journal of Mechanical Engineering, 2012, 48(19):29-34.